Journal: Head & Neck

Title: Surgical molecular navigation with a Ratiometric Activatable Cell Penetrating Peptide improves intraoperative identification and resection of small salivary gland cancers

Authors: Timon Hussain[1], MD; Elamprakash N. Savariar[2], PhD; Julio A. Diaz-Perez[1], MD; Karen Messer[3], PhD; Minya Pu[3], MA; Roger Y. Tsien[2, 4], PhD; Quyen T. Nguyen[1], MD/PhD

[1]Division of Head and Neck Surgery, University of California San Diego

[2]Department of Pharmacology, University of California San Diego

[3]Division of Biostatistics, Moores Cancer Center, University of California San Diego

[3]Howard Hughes Medical Institute, University of California San Diego

Running Title: RACPP-assisted molecular navigation improves tumor identification

Keywords:

Fluorescence Guided Surgery, Long Term Survival, Molecular Imaging, Molecular Navigation, RACPP

Preliminary results of this study were presented at the annual World Molecular Imaging Congress 2013, Savannah, GA, September 20, 2013.

Conflict of interest statement:

R.Y. Tsien, and Q.T. Nguyen are scientific advisors to Avelas Biosciences, which has licensed the ACPP technology from University of California Regents. No potential conflicts of interest were disclosed by the other authors.

Financial support:

1. NIH (NIBIB) R01 EB014929-01

08/08/2012 – 06/31/2016

PI: Quyen Nguyen

Title: Testing Fluorescently Labeled Probes for Nerve Imaging during Surgery

2. Burroughs-Wellcome Fund – (CAMS)

09/01/2009-08/31/2014

PI: Quyen Nguyen

Title: Testing surgery guided by molecular fluorescence imaging

3. NIH (NCI/NIBIB) 1R01CA158448-01A1

09/16/2011-08/31/2016

PI: Roger Tsien

Title: Injectable reporters to image tumors and guide resection

Corresponding Author: Timon Hussain, University of California San Diego, 9500 Gilman Drive La Jolla, CA 92093, Phone: 858-366-8472, Fax: 858-534-5270, E-mail: timon.hussain@gmail.com

Abstract

Background

We evaluated the use of intraoperative fluorescence guidance by enzymatically cleavable ratiometric activatable cell-penetrating peptide ($RACPP_{PLGC(Me)AG}$) containing Cy5 as a fluorescent donor and Cy7 as a fluorescent acceptor for salivary gland cancer surgery in a mouse model.

Methods

Surgical resection of small parotid gland cancers in mice was performed with fluorescence guidance or white light (WL) imaging alone. Tumor identification accuracy, operating time and tumor free survival were compared.

Results

RACPP guidance aided tumor detection (positive histology in 90% (27/30) vs. 48% (15/31) for WL, $p<0.001$). A ~25% ratiometric signal increase as the threshold to distinguish between tumor and adjacent tissue, yielded >90% detection sensitivity and specificity. Operating time was reduced by 54% ($p<0.001$), tumor free survival was increased with RACPP guidance ($p=0.025$).

Conclusions

RACPP provides real-time intraoperative guidance leading to improved survival. Ratiometric signal thresholds can be set according to desired detection accuracy levels for future RACPP applications.

Introduction

Currently, surgery is the primary treatment approach for most types of head and neck cancer.[1] Despite technical advancements such as improvements in ultrasound technology (US) and magnetic resonance imaging (MRI) which provide an improved pre-operative understanding of tumor location and characteristics,[2], the reported rate of positive or close surgical margins after head and neck cancer surgery remains considerable, ranging up to 43% depending on the location of the tumor[3, 4] even with intraoperative histological analysis of frozen sections. Surgeons have to rely on white light visualization and palpation to identify malignant tissue in an anatomical field where the immediate vicinity of vital structures such as the cranial nerves, the external and internal carotid arteries and the skull base prohibits an overly generous resection to ensure the removal of all malignant tissue. Surgical margin status correlates strongly with local recurrence and overall prognosis for head and neck cancer patients,[5, 6] emphasizing that there is a great need for tools to improve the intraoperative tumor identification and completeness of resection while preserving surrounding healthy tissue.[7]

Molecularly targeted fluorescently labeled imaging probes could potentially fill this void. They provide real time guidance for the surgeon by increasing the dynamic range of visual cues to differentiate between tumor and non-tumor tissue. Recently developed Ratiometric Activatable Cell Penetrating Peptides ($RACPP_{PLGC(Me)AG}$) contain Cy5 as far red fluorescent donor and Cy7 as near-infrared fluorescent acceptor.[13] Until enzymatic cleavage of the peptide sequence PLGC(Me)AG by matrix metalloproteinases (MMPs) 2 and 9 occurs, Cy5 is quenched in favor of Cy7 emission. Increased MMP 2 and 9 activity has been shown to be associated with many different types of cancer and we have previously shown tumor labeling in animal models of melanoma and breast cancer.[8] MMP 2 and 9 are also overexpressed in the microenvironment of human head and neck cancer variants,[9] and MMP2/9 mRNA has recently been reported to be increased in Head and Neck Squamous Cell Carcinoma (HNSCC) specimens from The

Cancer Genomic Atlas (TCGA) cohort compared to paired control normal tissue,[10] emphasizing the relevance of this technology in HNSCC.

_ENREF_12Upon cleavage by MMP 2 and 9, tissue retention of the Cy5 containing fragment occurs, while uncleaved peptides continue to emit fluorescence signal at Cy7 wavelength. Cancer to background contrast is generated based on the ratio of the two fluorescence emissions (Cy5/Cy7). Compared to single fluorophore probes, the ratiometric approach is relatively independent of interindividual differences in pharmacokinetics such as total probe uptake and washout, as well as thresholding. The rapidity of ratiometric change is particularly useful for surgical application of $RACPP_{PLGC(Me)AG}$. Malignant tissue (including primary tumors, distant metastases or lymph nodes) to background contrast is generated within 1-2 hours after systemic application, allowing for a real-time assessment of tumor margins and lymph node status.

In this study, we evaluated whether $RACPP_{PLGC(Me)AG}$ could improve the intraoperative identification and removal of head and neck tumors in a mouse model of parotid gland cancer. The parotid gland is a particularly delicate surgical field due to the immediate proximity of the facial nerve, making additional intraoperative guidance highly desirable to avoid over-resection while at the same ensuring tumor free surgical margins. We compared RACPP guided parotid gland cancer surgeries to procedures performed under WL alone and quantified operating time, sensitivity and specificity of the probe as well as long-term post-operative tumor-free survival. We also determined the ratiometric threshold for RACPP to allow for optimal tumor removal without over-resection of normal tissue.

[11][12, 13][14][8, 15][8, 15]

Materials and Methods

Animals

70 female Swiss-Webster mice (Jackson Laboratories, Bar Harbor, ME) were used in this study. All animal studies were approved by the UCSD Institutional Animal Care and Use Committee (protocol number S05536). 61 mice were included in the tumor removal study, 9 mice were used to establish the tumor model and for additional confocal microscopic imaging.

Establishment of the Tumor Model

To assess the kinetics of tumor growth after orthotopic injection of murine salivary gland cancer cells (SCA-9 clone 15, ATCC CRL-1734, American Type Culture Collection) and to determine the optimal cell injection dose to create small (1-2 mm) parotid gland cancers after 14d, $2.5x10^5$, $5x10^5$, $1x10^6$ or $2x10^6$ cells were injected into the right parotid glands of 8 syngeneic immune competent mice, n=2 per cell amount. Animals were anaesthetized with ketamine (50 mg/kg) and midazolam (1 mg/kg) for the procedure, and hair on the right side of the face was removed using depilatory cream (Nair, Church and Dwight Co., Ewing, NJ) Tumor growth patterns were observed by daily observation and palpation as well by autopsy and histological analysis after sacrifice of the mice 14 days after cell injection.

Molecular Imaging Probe

The ratiometric activatable cell penetrating peptide (RACPP) was synthesized as previously described.[11] In brief, H_2N-e_9-c(SS-tBu)o-PLGC(Me)AG-r_9-c-$CONH_2$ was reacted with Cy5-maleimide, subsequently treated with triethylphosphine to deprotect the tert-butylthio group, and then purified using high-performance liquid chromatography (HPLC). The purified compound was then reacted with m-dPEG_{12}-MAL (Quanta Biodesign). After completion of the reaction, Cy7 mono NHS ester (Cy7-NHS, GE Health Sciences) was added to get RACPP (Cy7-NH-e_9-c(peg_{12})-oPLGC(Me)AG-r_9-c(Cy5)). Then, the final compound was purified using C-18 reverse-phase HPLC.

Intraoperative Fluorescent Optical Imaging

Fluorescent intraoperative optical imaging was performed with a modified Olympus OV100 small animal imaging system (Cy5: 640 nm excitation/685 nm emission; Cy7 762 nm excitation/785 nm emission).

Survival Surgery

61 Swiss Webster mice with orthotopic salivary gland tumors generated by percutaneous injection of murine salivary gland cancer cells into the right parotid gland were included in the study. Prior to the surgical procedure, animals were either placed into the RACPP guidance arm (n=30) or the control group on which surgeries were performed with WL visualization alone (n=31).

Animals that were in the RACPP arm were briefly anaesthetized with inhalational isoflurane and intravenously injected with RACPP 2 hours before the beginning of the tumor removal surgery to allow for a sufficient MMP-cleavage induced accumulation in tumor and washout of nonspecific binding from non-tumor tissue.

For the surgeries, animals were injected with ketamine (150 mg/kg) and xylazine (10 mg/kg). Following facial hair removal with depilatory cream, a 2 cm infra-auricular skin incision was made and the skin retracted. Depending on their respective group allocation, salivary gland tumor identification was then attempted under WL or with RACPP guidance by surgically exploring the parotid gland and the surrounding infra-auricular region. The time from skin incision to tumor exposure was quantified for both groups. In the WL group, tissue which seemed most likely to be malignant in the parotid gland or the immediate vicinity of the gland was removed. In the RACPP guided group, fluorescently labeled foci in the same anatomical region were removed. All tissue was carefully excised in an attempt to preserve crucial anatomical structures, such as the facial nerve or the external jugular vein and its branches. However, if tumor had invaded those tissues, they were removed to ensure a maximal completeness of resection. Heat-cautery was used as needed to achieve hemostasis. After completion of tumor

resection, the skin was closed in a single layer. All animals were monitored daily for 5 days postoperatively to ensure adequate recovery from the surgical procedure.

Tumor Free Survival

After the initial 5-day postoperative observation period, all mice were monitored by research personnel blinded to the experimental condition once every four weeks for potential tumor recurrence by clinical inspection and manual palpation under a brief inhalational isoflurane anesthesia. If a deterioration in animal health was indicated by substantial weight loss, obvious discomfort or abnormal behavior, animals were sacrificed and removed from the study. For every clinical inspection, facial hair was removed with depilatory cream. If tumors were palpable or visible and the tumor diameter exceeded 5 mm, animals were sacrificed and the respective post-operative observation time point was considered the endpoint of tumor free survival. Animals, in which tumors smaller than 5 mm in diameter were clinically observed were further monitored. If the clinical tumor detection could be confirmed at the following inspection time points, the time point of first detection was considered the end-point of tumor free survival.

The final post-operative monitoring time point was 24 weeks after tumor removal surgery. At this point, all remaining mice were sacrificed. To definitely determine the presence or absence of tumor as previously assessed by the clinical inspection, tissue samples were collected from the parotid gland region for histological analysis. The majority of mice underwent a limited tissue collection procedure during which approximately 1x1x1 mm^3 biopsies were collected from the surgical field. This limited collection yielded inconclusive results, largely due to insufficient tissue. Consequently, the remaining mice (n = 18 (10 RACPP, 8 controls)) underwent an extensive tissue collection procedure including the tissue surrounding the parotid gland such as the infraauricular fat pad, connective tissue as well as lymph nodes. On average, 4 samples (one from each quadrant of the surgical field) of approximately

3x3x3 mm^3 were excised from the parotid gland region. Thus, the entire former surgical field could be histologically analyzed for potential tumor recurrence.

Histological Analysis

Tissue which was excised during the initial tumor removal surgery and during the postoperative follow up analysis, was immediately embedded in optimum tissue cutting (OCT) formulation (Tissue Tek, Thermo Fisher Scientific, Waltham, MA) and frozen. Multiple cryosections (8 µm) were obtained from every sample and histological analysis was conducted using hematoxylin and eosin (H&E) staining. A board certified pathologist blinded to the experimental conditions performed all histological analysis.

Microscopic Tumor Imaging

To further characterize fluorescent staining of malignant cells and their environment, additional *in vivo* confocal imaging was performed with a Nikon A1 upright confocal microscope **(Fig. 4)**.

Determination of ratiometric threshold

A receiver operator characteristic (ROC) analysis was performed to determine the accuracy of the ratiometric imaging probe and to identify an optimal threshold for the discrimination between tumor and healthy tissue. Cy5/Cy7 ratios were measured on images acquired during surgery from tumor tissue (n = 25), as well as tumor-free adjacent tissue (n = 34). Measurements were performed on ratiometric Cy5/Cy7 images acquired intraoperatively from mice which had later undergone an extensive tissue collection procedure followed by histological analysis to confirm the presence or absence of tumor. Cy5/Cy7 intensity ratios were measured in Image J by hand selecting regions of interest (ROIs) which had been histologically confirmed to be tumor as well as from immediately adjacent tissue in quadrants around the tumor confirmed to be tumor free. The mean pixel intensity values were measured. Cy5/Cy7

ratios were in all cases normalized to the Cy5/Cy7 background signal which was measured from skin tissue located outside the surgical bed.

Data Analysis

Statistical data analysis was performed using SigmaPlot software (Systat, San Jose, CA). An unpaired t-test was used to compare time to tumor exposure, Fisher's exact test was utilized to compare binary operative and postoperative histology results. A ROC analysis was conducted to analyze sensitivity and specificity of RACPP. The differences in tumor free survival assessed by clinical observation were compared with a log rank test; Kaplan-Meier curves were plotted for post-operative tumor free survival times. To accommodate possible errors in clinical assessment of tumor occurrence status in some mice, a simulation study was performed based on the observed error rates.

Results

Establishment of tumor model

Injection of $1x10^6$ salivary gland cancer cells into the right parotid gland region led to the development of tumors with a diameter of 1-2 mm after 14 days as confirmed by autopsy and histological analysis. This tumor size was determined to be suitable for the purpose of this study in which we attempted to evaluate the value of fluorescence guidance for the surgery of small salivary gland tumors. In order to simulate spontaneous tumor behavior, the malignant cells were injected through the skin without direct visualization of the gland in order to produce variability in the location of the cancer. This technique resulted in some tumors being located directly in the parotid gland, while others grew deeper within the masseter muscle or the infraauricular fat pad. A single surgeon blinded to the exact location of tumor injection performed all surgical resections.

Time to intraoperative tumor exposure

The operative time after skin incision to tumor exposure was quantified for both experimental groups. Tumor identification was significantly faster with ratiometric fluorescence imaging compared to white light alone ($p<0.001$**, Table 1**). With RACPP guidance, foci with high ratiometric values detected and surgically exposed in 5.1 minutes ± 1.8 (n=30). Under WL, the infrauricular region had to be extensively explored surgically and potentially malignant foci were exposed on average after 11.2 minutes ± 2.5 (n=31).

Intraoperative detection of malignant tissue

Intraoperative guidance with RACPPs significantly aided tumor identification compared to WL alone. 27/30 (90%) fluorescent foci excised were histologically positive for cancer, compared to 15/31 (48%) suspicious foci excised from the white light group ($p<0.001$, **Table 1, Figures 1 and 2**). Thus, the positive predictive value of the imaging probe was 90.0%, compared to 48.4% for WL. Sensitivity and specificity of the RACPP compared to WL in this experiment were calculated based on histology of tissue samples excised during the surgical procedure, which were assumed to be positive for tumor (test positive condition), as well as samples excised from the surgical bed postoperatively, which intraoperatively had been considered tumor-free (test negative condition). With RACPP guidance, 27/29 samples taken during the surgical procedure were correctly identified as tumor positive compared to 15/19 under WL. With RACPP guidance, 3/41 (7.31%) samples from the surgical bed were false positives, compared to 16/44 (36.4%) with WL. Sensitivity for RACPP was 93.1% (n = 27/29) vs. 79.0% for WL (n = 15/19) and specificity was 92.7% for RACPP (n = 38/41) vs. 63.6% for WL (n = 28/44) (**Figure 3A**).

Based on the ROC analysis (**Figure 3B**), RACPP showed very high accuracy for discriminating between tumor and adjacent non-tumor tissue (normal parotid gland, adipose tissue, connective tissue, muscle)

(AUC = 0.98 ± 0.02, p<0.0001). A ratiometric threshold in the range of 1.2 and 1.3 to discriminate between tumor and healthy tissue yielded the best sensitivity and specificity values. For example, a 1.265 fold increase in Cy5/Cy7 ratio between tumor and background resulted in 92.0% sensitivity and 91.2% specificity for tumor detection. This range of ratiometric change in fluorescence between tumor (Cy5/Cy7)/background (Cy5/Cy7) is consistent with previous report of RACPP performance.[11]

Tumor-Free Survival

Of the 61 mice on which tumor removal surgery was performed, 6 mice (2 in the RACPP group, 4 in WL group) died during the initial post-operative observation period or over the course of the follow-up period, most likely due to surgical complications, and these were excluded from further analysis.

Follow-up by clinical inspection and palpation

55 mice (28 RACPP group, 27 WL group) mice were assessed by clinical inspection and palpation with monthly follow up. The post-operative assessment indicated that tumor free survival was significantly increased (p = 0.025) when mice had received tumor removal surgery aided by fluorescence guidance rather than WL surgery (**Figure 5 A**). Over the course of the 6 months follow-up survival period, 4 mice (3 RACPP and 1 WL) developed tumors exceeding 5 mm in diameter and were sacrificed; time to tumor recurrence was noted for the survival analysis with time of death the day of sacrifice. The remaining mice were followed to 24 weeks after surgery, at which time they were sacrificed and tissue obtained from the surgical bed for and histological analyses.

Histological analysis

The final histological analysis after 6 months included tissue samples from 51 mice. The results from the initial limited tissue collection procedure (n=33) were inconclusive, largely due to insufficient tissue samples, showing detection of tumor in only 2/33 (6%) mice. A more extensive tissue collection procedure (3x3x3mm sample from each surgical quadrant) was performed on the remaining 18 mice (10

RACPP group, 8 controls). Histological results from these mice showed that 20% (2/10 mice) of mice which had undergone RACPP guided surgery were positive for tumor, compared to 50% (4/8 mice) of mice from the white light group. In 83% (15/18 mice) of cases, the histological findings confirmed the presence or absence of tumor as assessed by the clinical follow-up. Two mice (one RACPP and one WL) which had clinically shown signs of a parotid mass did not have histologically confirmed cancer, one mouse (RACPP group) showed positive histological evidence of cancer despite the absence of any clinically detectable mass. An analysis of tumor free survival for the subgroup of 18 mice (**Figure 5 B),** taking into account the clinical follow-up findings, and corrected according to the final histology results showed that RACPP guided surgery tended to increase tumor free survival and the two curves were well separated, but did not attain statistical significance (p=0.19), perhaps because of the limited sample size. After correcting tumor recurrence times and statuses for these three mice, using the whole data set of 55 mice, the RACPP group still had a significantly longer tumor free survival time than the control group (p=0.04).

We conducted a sensitivity analysis to address the concern that 33 mice did not go through the intensive histological examination, which had to be considered the gold standard to determine potential presence of tumor, leaving some uncertainty regarding tumor recurrence status. Among these mice there were 16 recurrences and 17 non-recurrences based on clinical assessment. We thus performed a simulation study to assess the robustness of the treatment effect after accommodating possible response assessment errors. From the 18 mice with certain tumor statuses, we estimated that the probability of mistreating tumor non-recurrence as recurrence was 28% (2/7); whereas the probability of mistreating tumor recurrence as non-recurrence was 9.1% (1/11). Using these rates, we randomly imputed 4 out of 16 observed recurrences to be true non-recurrences and set their survival times to be 24 weeks; we also randomly imputed 2 out of 17 the observed non-recurrences to be true recurrences and randomly chose their event times from the set of 4, 8, 12, 16, 20 and 24 weeks. We then combined these 33 mice with

imputed recurrence status together with the rest of the 23 mice with certain event statuses. A p-value was generated from this combined full data set. We repeated this process 1000 times and summarized p-values. The median of these p-values was 0.096 with interquartiles ranging from 0.03 and 0.13. Thus, the simulation analysis showed that the RACPP group was at least marginally significantly associated with longer tumor free survival, even accounting for possible estimated ascertainment error.

Discussion

The utilization of fluorescently labeled intraoperative molecular markers is still in the early stages of development but could substantially improve oncologic surgery.[12, 13] Fluorescent dyes and fluorescently labeled targeted probes have been shown to improve surgical results in human brain, liver and ovarian cancer surgery.[14-17] For head and neck cancer surgery, no intraoperative fluorescence guidance tools are in routine clinical use, but recent studies in animal models have suggested that fluorescence guidance can potentially be a valuable addition to existing treatment modalities.[18-20] A variety of potential tumor-specific targets for intraoperative optical imaging are evolving,[21] and for the intraoperative identification of head and neck cancers prior investigative approaches have focused primarily on antibody-based probes.[22-25][31-33] [34]While antibody-targeted approaches depend on adequate expression levels of highly specific markers, $RACPP_{PLGC(Me)AG}$ offers a more comprehensive approach because it is enzymatically activated by matrix metalloproteinases-2 and -9, which are associated with cancer invasion and metastasis across many different types of cancer.[26-29] _ENREF_28_ENREF_28Prior promising results in models of melanoma and breast cancer prompted us to assess the value intraoperative $RACPP_{PLGC(Me)AG}$ guidance for head and neck cancer surgery. Elevated MMP levels in the tumor microenvironment of head and neck cancers are a result of overexpression by multiple tumor-associated cell types, including immune cells,[30] reinforcing the necessity to perform the

experiments in immune competent mice; our particular orthotopic model also allowed for a long-term postoperative follow-up in this study.

Our results show that $RACPP_{PLGC(Me)AG}$ fluorescently labels small salivary gland cancers in mice with high specificity and sensitivity, hereby significantly aiding their intraoperative detection and surgical removal. The high specificity for labeling tumors two hours after probe injection emphasizes the value of the ratiometric imaging approach to minimize nonspecific signal generation, one of the key limiting factors of optical imaging approaches.[31, 32] Tumors generated in this study were only 1-2 mm in diameter at the time of surgery and not detectable clinically. Without fluorescence guidance, only 48% of the small lesions could be located compared to 90% in the RACPP guided group where the surgeon was guided to their location after skin incision. Our results suggest that intraoperative fluorescence guidance could be particularly valuable for the detection of clinically occult tumors of the head and neck. Especially when searching for an unknown primary in patients with metastatic head and neck cancer, diagnostic surgeries are required and large amounts of tissue have to be resected to yield positive results.[33, 34] In this study, an accurate detection and resection of small tumors was facilitated by intraoperative fluorescence guidance and time to tumor exposure was reduced by over 50%. Reducing operating time not only lowers associated cost but potentially favorably impacts postoperative patient morbidity, which has been shown to correlate with the extent of parotid gland surgery.[35] It should be noted no pre-operative US or MR imaging was performed in this study, though they are part of today's clinical staging process for salivary gland cancers. Both imaging modalities could have potentially provided additional pre-operative information in this particular model, offering high sensitivity and spatial resolution.[36, 37] ENREF 11 Pre-operative imaging however cannot provide the same level of guidance for the surgeon as real time imaging during the surgical resection as the orientation provided preoperatively is often lost after initial tissue dissection, particularly complicating the identification of small tumors.

Although the field of fluorescence guided surgery is gaining momentum with development of novel probes and instrumentation, one fundamental question remaining is how to determine the threshold for optimal tumor removal without over-resection of normal tissue. In this study, we leveraged the ratiometric nature of RACPP to address this issue by ROC, a commonly used tool to assess detection accuracy levels for imaging tools in cancer surgery.[38-40] The use of RACPP improved the intraoperative detection of very small tumors compared to WL with >90% sensitivity and specificity, and these levels corresponded to the detection accuracy for a ~25% ratiometric signal increase as the discrimination threshold between malignant and healthy tissue, as determined by postoperative receiver operator curve (ROC) analysis. By selecting a certain ratiometric signal threshold, sensitivity or specificity can be emphasized more strongly, depending on the preferred surgical outcome. We believe that this finding presents a significant advance in the field of molecular surgical navigation as it demonstrates proof of concept using ratiometric fluorescence to determine a threshold for the accuracy of tumor detection. In clinical practice, selection of a ratiometric threshold yielding high sensitivity could help to ensure tumor-free surgical margins while still allowing for an accurate resection without sacrificing healthy tissue. [11][44][45, 46][50-52]In this study the long-term (6 months) follow-up suggested increased tumor free survival for mice which had been operated with RACPP guidance compared to the mice which were operated on using white light alone, indicating that RACPP guidance enabled a complete tumor resection, i.e. clear surgical margins in the majority of mice.

It should be noted that the final histological analysis performed in this study to confirm our clinical findings demonstrated some ascertainment errors. The extensive histological analysis performed on a subgroup of mice confirmed the presence or absence of tumor as assessed by the clinical follow-up in 83% of cases and revealed that recurring or progressing tumors were mostly less than 3 mm in diameter and sometimes located deep in the tissue surrounding the parotid gland as well as adjacent lymph nodes. The small size of tumors detected by histological analysis after the 6 month follow-up period also

suggests that the findings of the clinical postoperative assessment can most likely not be attributed to the manual or visual detection of tumors in all cases. However, the extensive histological analysis showed that mice which had tumors regularly also had grossly enlarged cervical lymph nodes. We therefore hypothesize that these may have been manually detected during the clinical follow up period, indirectly but correctly indicating tumor prevalence. We note, however, that clinical assessment was blinded as to group status, supporting our findings of a significant difference. In addition, extensive and conservative simulation results incorporating the uncertainty of assessment generally supported our findings.

In conclusion, we show that RACPP is a promising optical molecular imaging probe with very sensitive and specific intraoperative tumor visualization. The broad applicability for many types of cancer should benefit future clinical translation of this imaging probe. In head and neck cancer surgery in particular, the high accuracy in labeling small tumors can be very valuable to aid identification and resection while reducing operating time and limiting damage to surrounding important structures. Post-operative follow-up data suggests that RACPP may increase tumor free survival after surgery by facilitating complete tumor resection.

Acknowledgements:

The authors thank the members of our laboratory for discussions and comments on the manuscript; P. Steinbach, N. Nashi and P. Arcaria for technical assistance.

References

1. Argiris A, Karamouzis MV, Raben D, Ferris RL. Head and neck cancer. Lancet 2008;371(9625):1695-709.
2. Lee YY, Wong KT, King AD, Ahuja AT. Imaging of salivary gland tumours. European journal of radiology 2008;66(3):419-36.
3. Woolgar JA, Triantafyllou A. A histopathological appraisal of surgical margins in oral and oropharyngeal cancer resection specimens. Oral oncology 2005;41(10):1034-43.
4. McMahon J, O'Brien CJ, Pathak I, et al. Influence of condition of surgical margins on local recurrence and disease-specific survival in oral and oropharyngeal cancer. The British journal of oral & maxillofacial surgery 2003;41(4):224-31.
5. Cook JA, Jones AS, Phillips DE, Soler Lluch E. Implications of tumour in resection margins following surgical treatment of squamous cell carcinoma of the head and neck. Clinical otolaryngology and allied sciences 1993;18(1):37-41.
6. Haque R, Contreras R, McNicoll MP, Eckberg EC, Petitti DB. Surgical margins and survival after head and neck cancer surgery. BMC ear, nose, and throat disorders 2006;6:2.
7. Keereweer S, Sterenborg HJ, Kerrebijn JD, Van Driel PB, Baatenburg de Jong RJ, Lowik CW. Image-guided surgery in head and neck cancer: current practice and future directions of optical imaging. Head & neck 2012;34(1):120-6.
8. Nguyen QT, Olson ES, Aguilera TA, et al. Surgery with molecular fluorescence imaging using activatable cell-penetrating peptides decreases residual cancer and improves survival. Proceedings of the National Academy of Sciences of the United States of America 2010;107(9):4317-22.
9. Rosenthal EL, Matrisian LM. Matrix metalloproteases in head and neck cancer. Head & neck 2006;28(7):639-48.
10. Hauff SJ, Raju SC, Orosco RK, et al. Matrix-Metalloproteinases in Head and Neck Carcinoma-Cancer Genome Atlas Analysis and Fluorescence Imaging in Mice. Otolaryngology--head and neck surgery : official journal of American Academy of Otolaryngology-Head and Neck Surgery 2014.
11. Savariar EN, Felsen CN, Nashi N, et al. Real-time in vivo molecular detection of primary tumors and metastases with ratiometric activatable cell-penetrating peptides. Cancer research 2013;73(2):855-64.
12. Nguyen QT, Tsien RY. Fluorescence-guided surgery with live molecular navigation - a new cutting edge. Nature reviews Cancer 2013.
13. Frangioni JV. New technologies for human cancer imaging. Journal of clinical oncology : official journal of the American Society of Clinical Oncology 2008;26(24):4012-21.

14. Stummer W, Pichlmeier U, Meinel T, et al. Fluorescence-guided surgery with 5-aminolevulinic acid for resection of malignant glioma: a randomised controlled multicentre phase III trial. The lancet oncology 2006;7(5):392-401.
15. Widhalm G, Wolfsberger S, Minchev G, et al. 5-Aminolevulinic acid is a promising marker for detection of anaplastic foci in diffusely infiltrating gliomas with nonsignificant contrast enhancement. Cancer 2010;116(6):1545-52.
16. Gotoh K, Yamada T, Ishikawa O, et al. A novel image-guided surgery of hepatocellular carcinoma by indocyanine green fluorescence imaging navigation. Journal of surgical oncology 2009;100(1):75-9.
17. van Dam GM, Themelis G, Crane LM, et al. Intraoperative tumor-specific fluorescence imaging in ovarian cancer by folate receptor-alpha targeting: first in-human results. Nature medicine 2011;17(10):1315-9.
18. Reddy NP, Miyamoto S, Araki K, et al. A novel orthotopic mouse model of head and neck cancer with molecular imaging. The Laryngoscope 2011;121(6):1202-7.
19. Miyamoto S, Sperry S, Yamashita T, Reddy NP, O'Malley BW, Jr., Li D. Molecular imaging assisted surgery improves survival in a murine head and neck cancer model. International journal of cancer Journal international du cancer 2012;131(5):1235-42.
20. Loja MN, Luo Z, Greg Farwell D, et al. Optical molecular imaging detects changes in extracellular pH with the development of head and neck cancer. International journal of cancer Journal international du cancer 2013;132(7):1613-23.
21. Keereweer S, Kerrebijn JD, van Driel PB, et al. Optical image-guided surgery--where do we stand? Molecular imaging and biology : MIB : the official publication of the Academy of Molecular Imaging 2011;13(2):199-207.
22. Kulbersh BD, Duncan RD, Magnuson JS, Skipper JB, Zinn K, Rosenthal EL. Sensitivity and specificity of fluorescent immunoguided neoplasm detection in head and neck cancer xenografts. Archives of otolaryngology--head & neck surgery 2007;133(5):511-5.
23. Rosenthal EL, Kulbersh BD, Duncan RD, et al. In vivo detection of head and neck cancer orthotopic xenografts by immunofluorescence. The Laryngoscope 2006;116(9):1636-41.
24. Gleysteen JP, Newman JR, Chhieng D, Frost A, Zinn KR, Rosenthal EL. Fluorescent labeled anti-EGFR antibody for identification of regional and distant metastasis in a preclinical xenograft model. Head & neck 2008;30(6):782-9.
25. Heath CH, Deep NL, Sweeny L, Zinn KR, Rosenthal EL. Use of panitumumab-IRDye800 to image microscopic head and neck cancer in an orthotopic surgical model. Annals of surgical oncology 2012;19(12):3879-87.
26. Jinga DC, Blidaru A, Condrea I, et al. MMP-9 and MMP-2 gelatinases and TIMP-1 and TIMP-2 inhibitors in breast cancer: correlations with prognostic factors. Journal of cellular and molecular medicine 2006;10(2):499-510.
27. Maatta M, Soini Y, Liakka A, Autio-Harmainen H. Differential expression of matrix metalloproteinase (MMP)-2, MMP-9, and membrane type 1-MMP in hepatocellular and pancreatic adenocarcinoma: implications for tumor progression and clinical prognosis. Clinical cancer research : an official journal of the American Association for Cancer Research 2000;6(7):2726-34.
28. Bauvois B. New facets of matrix metalloproteinases MMP-2 and MMP-9 as cell surface transducers: outside-in signaling and relationship to tumor progression. Biochimica et biophysica acta 2012;1825(1):29-36.
29. Egeblad M, Werb Z. New functions for the matrix metalloproteinases in cancer progression. Nature reviews Cancer 2002;2(3):161-74.
30. Curry JM, Sprandio J, Cognetti D, et al. Tumor microenvironment in head and neck squamous cell carcinoma. Seminars in oncology 2014;41(2):217-34.

31. Keereweer S, Mol IM, Vahrmeijer AL, et al. Dual wavelength tumor targeting for detection of hypopharyngeal cancer using near-infrared optical imaging in an animal model. International journal of cancer Journal international du cancer 2012;131(7):1633-40.
32. Baeten J, Haller J, Shih H, Ntziachristos V. In vivo investigation of breast cancer progression by use of an internal control. Neoplasia 2009;11(3):220-7.
33. Waltonen JD, Ozer E, Schuller DE, Agrawal A. Tonsillectomy vs. deep tonsil biopsies in detecting occult tonsil tumors. The Laryngoscope 2009;119(1):102-6.
34. Nagel TH, Hinni ML, Hayden RE, Lott DG. Transoral laser microsurgery for the unknown primary: role for lingual tonsillectomy. Head & neck 2014;36(7):942-6.
35. Koch M, Zenk J, Iro H. Long-term results of morbidity after parotid gland surgery in benign disease. The Laryngoscope 2010;120(4):724-30.
36. Yabuuchi H, Fukuya T, Tajima T, Hachitanda Y, Tomita K, Koga M. Salivary gland tumors: diagnostic value of gadolinium-enhanced dynamic MR imaging with histopathologic correlation. Radiology 2003;226(2):345-54.
37. Massoud TF, Gambhir SS. Molecular imaging in living subjects: seeing fundamental biological processes in a new light. Genes & development 2003;17(5):545-80.
38. Hricak H, Wang L, Wei DC, et al. The role of preoperative endorectal magnetic resonance imaging in the decision regarding whether to preserve or resect neurovascular bundles during radical retropubic prostatectomy. Cancer 2004;100(12):2655-63.
39. Junaid M, Choudhary MM, Sobani ZA, et al. A comparative analysis of toluidine blue with frozen section in oral squamous cell carcinoma. World journal of surgical oncology 2012;10:57.
40. Roder C, Bender B, Ritz R, et al. Intraoperative visualization of residual tumor: the role of perfusion-weighted imaging in a high-field intraoperative magnetic resonance scanner. Neurosurgery 2013;72(2 Suppl Operative):ons151-8; discussion ons158.

Table

Summary of operative results

Group	*No. per group*	*Time to tumor exposure after skin incision ± SD*	*Presence of cancer in resected tissue*
RACPP	30	5.1 min ± 1.8	27/30 (90%)
WL	31	11.2 min ± 2.5	15/31 (48%)
		p < 0.0001	*p = 0.0007*

Table 1: Summary of operative results. Time to exposure of potentially malignant tissue foci after skin incision was significantly reduced with RACPP guidance compared to procedures performed under white light (WL) alone. Fluorescence guidance also significantly aided the surgeon in identifying the small malignant lesions, indicated by the results of the histological analysis of excised tissue samples.

Figure Legends

Figure 1 A. Intraoperative view of the surgical bed after skin incision. **B. Cy5** fluorescence signal was visible through overlying healthy tissue and guided the surgeon to the location of the small tumor. **C.** The ratiometric image depicting Cy5/Cy7 ratios further aids the visual identification of the tumor. Here

the tumor clearly shows the highest Cy5 intensity and low Cy7 intensity (i.e. high Cy5/Cy7 ratio, depicted in red) providing high detection specificity.

D. Intraoperative view of the surgical bed after dissection of overlying connective tissue and parts of the parotid gland. **E.** Fluorescence signal helps the surgeon to identify the extent of the tumor, enabling a more complete resection. Compared to the white light image the assessment of the extent of the tumor is easier with the fluorescence signal. **F.** Ratiometric imaging further aids the visual identification by indicating the location of highest Cy5/Cy7 ratio. The ratio scale bars indicate the level of Cy5/Cy7 ratio. Scale bars: 5 mm.

Figure 2 All excised tissue samples were analyzed by a pathologist blinded to experimental conditions after hematoxylin and eosin staining. **A, B.** Histological section of normal parotid gland tissue from a negative tissue sample **C, D.** Tumor positive tissue sample. Scale bars: 100 µm.

Figure 3 A. Based on histological analysis of tissue samples excised during the surgical procedure and postoperatively, RACPP increases the accuracy of intraoperative tumor detection compared to WL. **B.** Receiver Operating Characteristic (ROC) Analysis illustrates the high accuracy of the RACPP for tumor detection (AUC = 0.98, $p<0.0001$). Selecting a ratio threshold in the range of 1.2 and 1.3 to discriminate between tumor and healthy tissue yields the best trade-off between sensitivity and specificity.

Figure 4 A. Macroscopic ratiometric image of a large parotid gland tumor (white stippled outline) imaged after RACPP injection. Red pseudocolor indicates high Cy5/Cy7 ratio, while blue/green color indicates low Cy5/Cy7 ratio. The overlying skin has been retracted from the tumor and shows high ratio due to cancer invasion (white arrows). Scale bar: 5 mm. **B.** Area of the anterior tumor border (white asterisk in A) imaged at higher magnification with confocal microscopy. Individual cells are labeled with

higher Cy5/Cy7 ratio than others and can be distinguished from fat vacuoles (white asterisks in B) and healthy surrounding tissue (white stippled outline) around the tumor. Scale bar: 100 µm.

Figure 5 A. Kaplan-Meier curve showing post-operative tumor free survival, as assessed by monthly clinical inspection and palpation, showed significant improvement for mice whose surgical procedures were performed with RACPP guidance (n=28, stippled line) compared to surgeries performed under white light alone (n=27, solid line, p=0.025). **B.** A separate Kaplan-Meier analysis of tumor free survival was performed for the subgroup of mice (n=18) which had undergone an extensive tissue collection procedure and histological analysis six months after surgery. Taking clinical follow-up findings and final histology into account, RACPP guidance (n=10) tended to improve tumor free survival compared to white light surgery (n=8). Subgroup results were not statistically significant, due to limited sample size (p=0.19).

Fig. 1

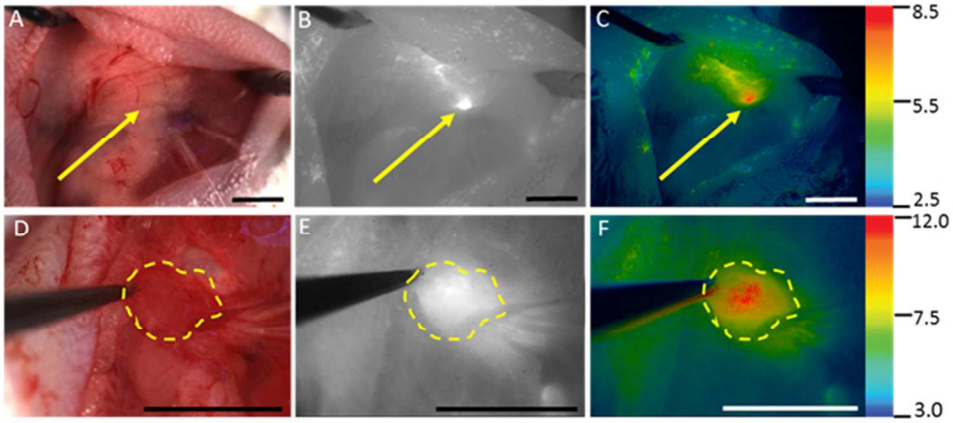

Figure 1: A, B, C. Intraoperative view of the surgical bed after skin incision. Fluorescence signal was visible through overlying healthy tissue and guided the surgeon to the location of the small tumor which cannot be identified immediately under white light (A). The malignant focus is visible with the Cy5 intensity visualization (B). In B there is some increased Cy5 uptake in the skin as well. The ratiometric image depicting Cy5/Cy7 ratios (C) further aids the visual identification of the tumor. Here the tumor clearly shows the highest Cy5 intensity and low Cy7 intensity (i.e. high Cy5/Cy7 ratio, depicted in red) providing high detection specificity. The ratio scale bar indicates the level of Cy5/Cy7 ratio. Scale bars: 5 mm.
D, E, F. Intraoperative view of the surgical bed after dissection of overlying connective tissue and parts of the parotid gland. Fluorescence signal helps the surgeon to identify the extent of the tumor, enabling a more complete resection. Compared to the white light image (A), the assessment of the extent of the tumor is easier with the fluorescence signal (B). Ratiometric imaging (C) further aids the visual identification by indicating the location of highest Cy5/Cy7 ratio. The ratio scale bar indicates the level of Cy5/Cy7 ratio. Scale bars: 5 mm.
188x90mm (96 x 96 DPI)

Fig. 2

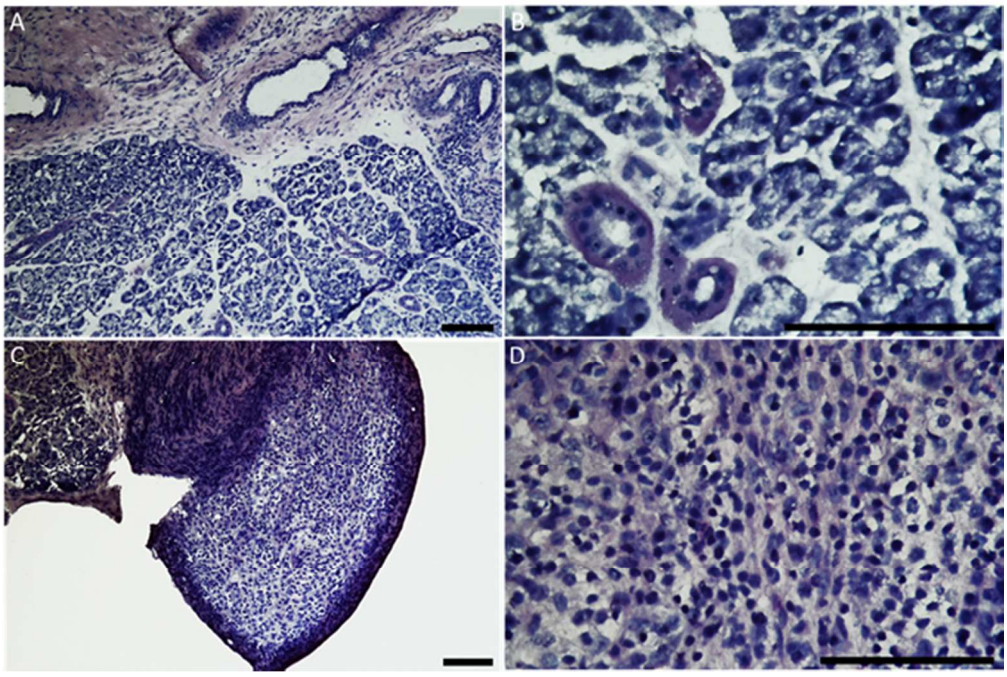

Figure 2: All excised tissue samples were analyzed by a pathologist blinded to experimental conditions after hematoxylin and eosin staining. Histological section of normal parotid gland tissue from a negative tissue sample (A and B) compared to a tumor positive tissue sample (C and D). Scale bars: 100 μm.
179x129mm (96 x 96 DPI)

Fig. 3

A

Intraoperative Accuracy of Tumor Detection

Group	*Sensitivity*	*Specificity*
RACPP (n=70 tissue samples)	93.1%	92.7%
WL (n=63 tissue samples)	78.9%	63.6%

B

Receiver Operating Characteristic Analysis

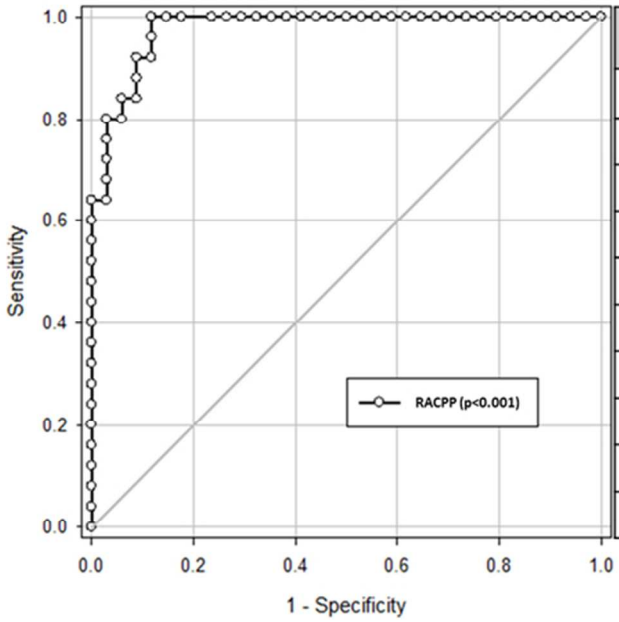

Ratio Threshold	*Sensitivity*	*Specificity*
1.2	1	0.77
1.203	1	0.82
1.205	1	0.85
1.221	1	0.88
1.241	0.96	0.88
1.255	0.92	0.88
1.265	0.92	0.91
1.266	0.88	0.91
1.272	0.84	0.91
1.301	0.84	0.94

Figure 3: A. Based on histological analysis of tissue samples excised during the surgical procedure and postoperatively, RACPP increases the accuracy of intraoperative tumor detection compared to WL. B. Receiver Operating Characteristic (ROC) Analysis illustrates the high accuracy of the RACPP for tumor detection (AUC = 0.98, p<0.0001). Selecting a ratio threshold in the range of 1.2 and 1.3 to discriminate between tumor and healthy tissue yields the best trade-off between sensitivity and specificity.
191x171mm (96 x 96 DPI)

Fig. 4

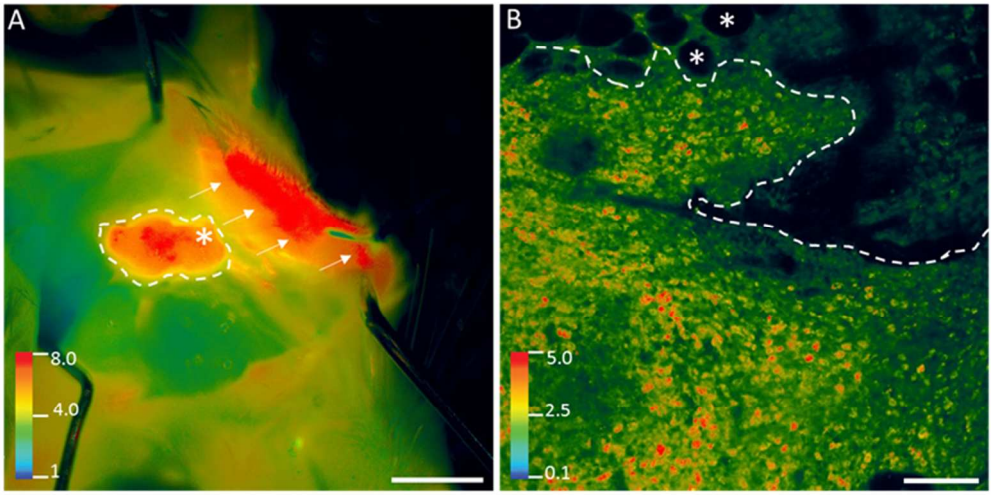

Figure 4: A. Macroscopic ratiometric image of a large parotid gland tumor (white stippled outline) imaged after RACPP injection. Red pseudocolor indicates high Cy5/Cy7 ratio, while blue/green color indicates low Cy5/Cy7 ratio. The overlying skin has been retracted from the tumor and shows high ratio due to cancer invasion (white arrows). Scale bar: 5 mm. B shows an area of the anterior tumor border (white asterisk in A) imaged at higher magnification with confocal microscopy. Individual cells are labeled with higher Cy5/Cy7 ratio than others and can be distinguished from fat vacuoles (white asterisks in B) and healthy surrounding tissue (white stippled outline) around the tumor. Scale bar: 100 μm.
208x112mm (96 x 96 DPI)

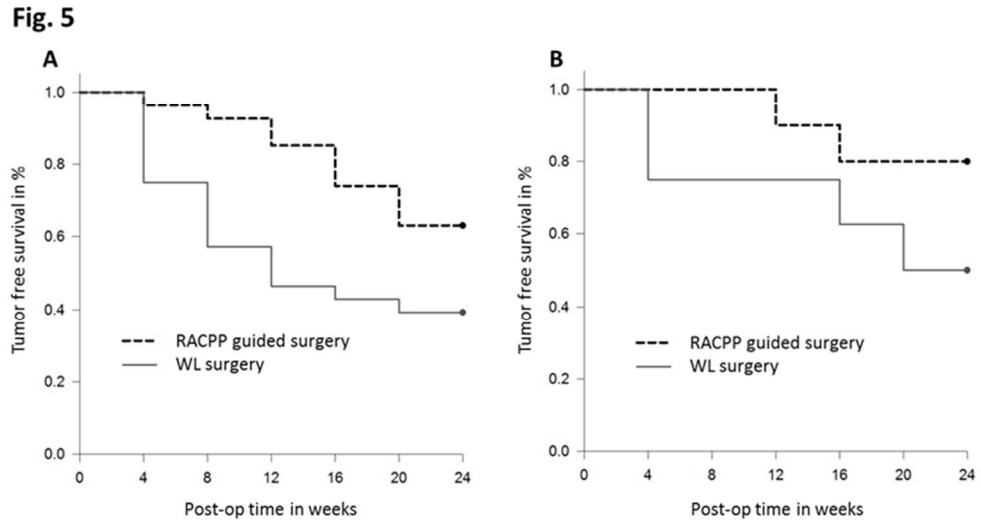

Figure 5: A. Kaplan-Meier curve showing post-operative tumor free survival, as assessed by monthly clinical inspection and palpation, showed significant improvement for mice whose surgical procedures were performed with RACPP guidance (n=28, stippled line) compared to surgeries performed under white light alone (n=27, solid line, p=0.025). B. A separate Kaplan-Meier analysis of tumor free survival was performed for the subgroup of mice (n=18) which had undergone an extensive tissue collection procedure and histological analysis six months after surgery. Taking clinical follow-up findings and final histology into account, RACPP guidance (n=10) tended to improve tumor free survival compared to white light surgery (n=8). Subgroup results were not statistically significant, due to limited sample size (p=0.19).
218x117mm (96 x 96 DPI)